Published in "PhysicalReview A 78:032501,2008"
which should be cited to refer to this work.

Lifetime studies of Cs*He$_N$ exciplexes in solid ^{4}He

P. Moroshkin, A. Hofer, V. Lebedev, and A. Weis
Département de Physique, Université de Fribourg, Chemin du Musée 3, 1700 Fribourg, Switzerland[*]

We present time-resolved measurements of the laser-induced fluorescence from Cs atoms and Cs*He$_N$ exciplexes in a solid ^{4}He matrix. The linear Cs*He$_{N=2}$ exciplex is strongly quenched by a radiationless transformation into a ring-shaped Cs*He$_{N=6,7}$ exciplex, which decays radiatively with a lifetime of 88 ± 2 ns. The analysis of this lifetime provides information on the formation rate of Cs*He$_{N=6,7}$ and on perturbations of the electronic states of the Cs atom by the bound helium atoms.

PACS number(s): 32.70.Cs, 33.50.−j, 67.80.B−

I. INTRODUCTION

Complexes formed by helium atoms bound by van der Waals forces to an excited alkali-metal atom, so-called exciplexes, have been studied extensively in the past 10 years. Exciplexes were observed in liquid He and in cold He gas [1–3], on He nanodroplets [4–9], and in solid He [10–12]. The exciplexes are usually detected via their laser-induced fluorescence following the resonant excitation of an atomic transition. The characteristic feature of exciplex emission is the strong redshift of the fluorescence radiation compared to the corresponding atomic absorption wavelength. For instance, the Cs*He$_{N=6,7}$ exciplex, which is formed after excitation at 800 nm, emits fluorescence at 1400 nm (Fig. 1). Time-resolved fluorescence was observed for the Na*He [4] and K*He [6] diatomic exciplexes (excimers) formed on the surface of He droplets. In both cases the measured fluorescence decay time was slightly longer than the radiative lifetime of the corresponding atomic excited state.

The radiative lifetime τ of an excited state $|n_e, L_e, J_e\rangle$, decaying to a ground state $|n_g, L_g, J_g\rangle$, is related to the transition frequency ω_0 and the matrix element $D = \langle n_g, L_g, J_g | d | n_e, L_e, J_e \rangle$ of the electric-dipole operator d via

$$\frac{1}{\tau} = \frac{\omega_0^3 |D|^2}{3(2J_e + 1)\pi\epsilon_0 \hbar c^3}. \quad (1)$$

Here n, L, and J refer to the principal quantum number, the orbital angular momentum quantum number, and the total electronic momentum quantum number, respectively. The experimental lifetimes of Na*He [4] and K*He [4,6] were explained by assuming that the dipole matrix element $|D|$ is not affected by the interaction with the He atoms, so that only the redshift of the transition is responsible for the lengthening of the lifetime.

In recent publications [10,11] we have presented spectroscopic studies of Cs*He$_N$ exciplexes produced by laser excitation of Cs atoms isolated in a solid ^{4}He matrix. A typical fluorescence spectrum induced by laser excitation at the wavelength (800 nm) of the $6S_{1/2} \rightarrow 6P_{3/2}$ transition of Cs in solid He is shown in Fig. 1. The laser-excited $6P_{3/2}$ state is completely quenched and does not emit any fluorescence on the $6P_{3/2} \rightarrow 6S_{1/2}$ transition. However, fluorescence appears at 879 nm, corresponding to the $6P_{1/2} \rightarrow 6S_{1/2}$ (D_1) transition (peak *a* in Fig. 1). Besides this atomic emission the fluorescence spectrum contains two spectral features corresponding to emission by the Cs($6P_{3/2}$)He$_{N=2}$ exciplex at 950 nm (peak *b*) and by the Cs($6P_{1/2}$)He$_N$ ($N=6$ or 7 [10,11]) exciplex at 1400 nm (peak *c*). When the $6P_{1/2}$ state is directly excited by the laser tuned to the D_1 transition under otherwise identical conditions, the fluorescence is strongly dominated by the atomic D_1 emission. As discussed in [11], exciplex formation from the $6P_{1/2}$ state proceeds via a strongly suppressed tunneling transition. Nevertheless, very weak emission lines of the Cs($6P_{1/2}$)He$_{N=2}$ and Cs($6P_{1/2}$)He$_{N=6,7}$ exciplexes could be observed.

In this paper we present first lifetime measurements of the Cs*He$_N$ exciplexes in solid He produced via D_2 and D_1 excitation. The large Cs*He$_{N=6,7}$ complex decays by a radiative transition to the ground state, while the Cs*He$_{N=2}$ complex is strongly quenched by a radiationless process, most likely by the formation of Cs*He$_{N=6,7}$.

II. EXPERIMENT

The lifetime measurements were performed on Cs atoms and Cs*He$_N$ exciplexes trapped in a hcp ^{4}He crystal at $p = 30$ bars. The helium crystal is grown in a copper cell with

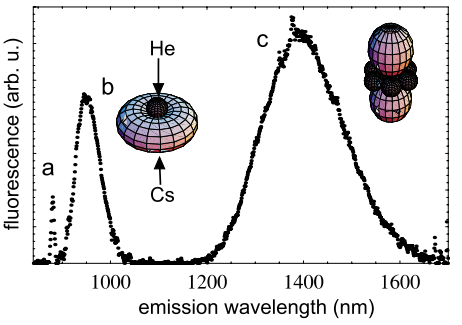

FIG. 1. (Color online) Emission spectrum recorded after laser excitation of Cs atoms trapped in hcp solid He to the $6P_{3/2}$ state. The observed spectral features are *a*, D_1 atomic emission at 879 nm; *b*, Cs*He$_{N=2}$ exciplex emission; and *c*, Cs*He$_{N=6,7}$ exciplex emission. The electronic density distributions of the exciplexes are shown in the insets.

[*]www.unifr.ch/physics/frap/

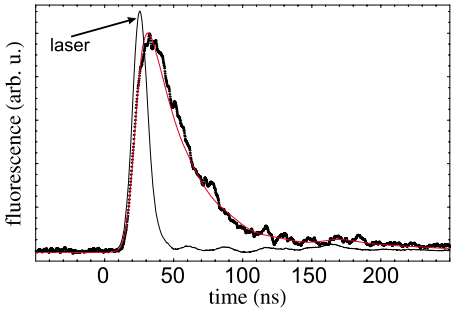

FIG. 2. (Color online) Fluorescence pulse (black dots) of D_1 emission following D_2 excitation (peak *a* of Fig. 1). The thin black curve is the pulse shape of the excitation laser recorded by the same system. The red curve is a convolution of the laser pulse shape and an exponential decay curve with a decay constant $\tau(6P_{1/2})$ of 29.3 ns. Experimental conditions: T=1.5 K, p=31 bars.

an inner volume of 170 cm^3 by applying pressure from an external He reservoir. The cell is immersed in superfluid He cooled to 1.5 K by pumping on the helium bath. Cs atoms are implanted in the He crystal by means of laser ablation with a pulsed frequency-doubled Nd:YAG laser focused onto a solid Cs target at the bottom of the pressure cell. Details of the implantation procedure were presented earlier [13,14].

The trapped Cs atoms are excited by the idler beam of a pulsed optical parametric oscillator (OPO) with a pulse width of 10 ns. Fluorescence light is collected at right angles with respect to the excitation laser beam and dispersed in a spectrograph. The time-resolved fluorescence at a chosen wavelength is recorded either with a photomultiplier (for wavelengths below 950 nm) or with an InGaAs photodiode (for longer wavelengths). The pulse shapes of the fluorescence are stored in a digital oscilloscope with a time resolution of 1 ns.

We recorded time-resolved fluorescence pulses induced by laser excitation at 800 nm (atomic D_2 transition) or at 850 nm (atomic D_1 transition) with the spectrograph set to each of the three emission peaks of Fig. 1. The results are shown in Figs. 2–4, respectively. On all three time traces we also show the laser pulse recorded with the same detection system. The time resolution depends on the detector used and is ≈1 ns for photomultiplier detection (Figs. 2 and 3) and ≈50 ns for InGaAs photodiode detection (Fig. 4).

The time-dependent atomic D_1 fluorescence at 879 nm (peak *a* in Fig. 1) is shown in Fig. 2. The observed fluorescence pulse is fitted with the convolution of the recorded laser pulse shape and an exponential decay, and the result shown as a solid red curve. The exponential decay constant $\tau(6P_{1/2})$ was found to be 29.3 ± 0.2 ns and agrees well with the radiative lifetime of the $6P_{1/2}$ state of Cs in solid He measured in our recent experiment using correlated single-photon counting [15].

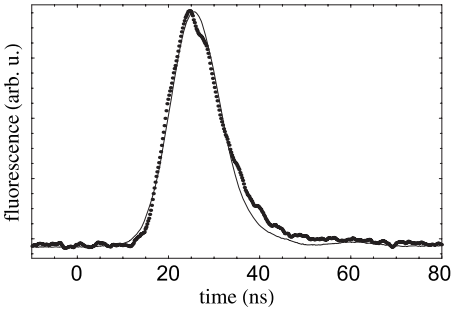

FIG. 3. Pulse shape of the Cs*He$_{N=2}$ fluorescence (black dots) following D_2 excitation (peak *b* of Fig. 1) measured with a photomultiplier. The thin black line is the laser pulse shape.

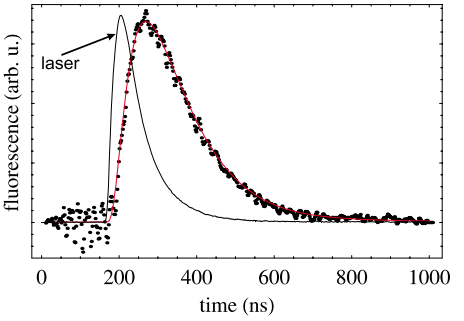

FIG. 4. (Color online) Pulse shape of the Cs*He$_{N=6,7}$ fluorescence (black dots) following D_2 excitation (peak *c* of Fig. 1) measured with a InGaAs photodiode. The thin black line is the recorded laser pulse shape, which differs from the one shown in Fig. 3 due to the slower response of the photodiode. The fitted red curve is the convolution of the laser pulse with an exponential decay.

The emission of the Cs($6P_{3/2}$)He$_{N=2}$ exciplex (peak *b* in Fig. 1) following D_2 excitation is shown in Fig. 3. The fluorescence pulse almost matches the laser pulse shape, but has a slightly longer tail, from which we can only assign an upper limit of ≲5 ns to the lifetime τ(Cs*He$_{N=2}$) of this complex. This short lifetime differs substantially from related measurements [4,5] on Na*He and K*He, for which lifetimes exceeding the corresponding atomic lifetimes were found. We have also measured the fluorescence pulse shapes from the same Cs($6P_{1/2}$)He$_{N=2}$ exciplex formed after exciting Cs atoms on the D_1 line at 850 nm. In that case the fluorescence of exciplexes is two orders of magnitude weaker than the atomic D_1 fluorescence [11]. The observed fluorescence pulse has the same shape as the pulse after D_2 excitation, but its signal-to-noise ratio is much smaller. From the observations we conclude that this Cs($6P_{1/2}$)He$_{N=2}$ exciplex is strongly quenched by a radiationless process.

Figure 4 shows the pulse shape of the Cs*He$_{N=6,7}$ emission (peak *c* in Fig. 1). Due to the lower time resolution of the detector, the laser pulse and the rising edge of the fluorescence pulse are unresolved. However, the exponential decay of the fluorescence is very long and is well resolved. A separate measurement with a faster photodiode produced a similar decay curve, but with a worse signal-to-noise ratio, so that we preferred to use the slower detector for quantitative measurements. By fitting the observed pulse shape with the convolution of laser pulse shape and an exponential decay, we obtained a lifetime τ(Cs*He$_{N=6,7}$)=88 ± 2 ns for the Cs*He$_{N=6,7}$ exciplex.

III. DISCUSSION

A. Radiative lifetimes of Cs*He$_N$ exciplexes

The smaller triatomic Cs*He$_{N=2}$ exciplex has a linear structure with the Cs atom halfway between the He atoms.

The larger Cs*$He_{N=6,7}$ exciplex consists of a ring of N He atoms around the Cs atom. The Cs-He separations in both complexes are approximately 3.5 Å. In [11] we have modeled the electronic structure of the Cs*He_N exciplexes using Cs-He pair potentials. The model predicts the observed fluorescence spectra of the exciplexes reasonably well, even though it ignores the interaction of the exciplex with the surrounding helium bulk. For the larger exciplex the comparison of the experimental spectra with the model predictions did not allow us to ascertain whether $N=6$ or $N=7$ [11].

1. Lifetime of the Cs*$He_{N=6,7}$ *exciplex*

The electronic state of the Cs atom in the exciplex is perturbed by the interaction with the He atoms, and the perturbed state can be represented as a superposition of energy eigenstates of the free Cs atom. In the following discussion the symbols L, S, and J denote the orbital, spin, and total angular momenta of the valence electron with projections M_L, M_S, and M_J, respectively. We use the notation $|\widetilde{nL_J, M_J}\rangle$ and $|nL, M_L, M_S\rangle$ to denote the perturbed states and the L-S decoupled unperturbed basis states, respectively.

The total Hamiltonian H includes the spin-orbit coupling H_{SO} in the Cs atom and the perturbation $V_{\text{Cs-He}}$. We use an expansion of $V_{\text{Cs-He}}$ into spherical harmonics:

$$H = H_{SO} + \sum_{k,q} V_{k,q}(r) Y_q^{(k)}(\theta,\phi). \tag{2}$$

The structure of the perturbation Hamiltonian $V_{\text{Cs-He}}$ reflects the symmetry of the distribution of He atoms which belongs to the D_{6h} or D_{7h} symmetry group for $N=6$ or 7, respectively. The reflection symmetry of the Hamiltonian with respect to the x-y plane implies that only even terms give a nonzero contribution. The rotation symmetry requires that only the terms with $q=0, \pm N$ be nonzero. For the terms with $k<N$, only those with $q=0$ are nonzero. For $N=6$ we obtain

$$H = H_{SO} + \sum_{k=0,2,4} V_{k,0} Y_0^{(k)} + \sum_{\kappa=3}^{\infty} \sum_{q=0,\pm 6} V_{2\kappa,q} Y_q^{(2\kappa)} \tag{3}$$

and, for $N=7$,

$$H = H_{SO} + \sum_{k=0,2,4,6} V_{k,0} Y_0^{(k)} + \sum_{\kappa=4}^{\infty} \sum_{q=0,\pm 7} V_{2\kappa,q} Y_q^{(2\kappa)}. \tag{4}$$

The He atoms in the exciplex are arranged in such a way that there is a minimal overlap of their closed electronic shells and the valence electron of the Cs atom. The interaction in that case is mostly due to the attractive van der Waals force and the perturbation of the Cs atom is rather weak. Restricting the basis to the six $|6P, M_L, M_S\rangle$ states, we have shown [11] by a diagonalization of H that the Cs-He interaction in the Cs*$He_{N=6,7}$ exciplex decouples the spin angular momentum almost completely from the orbital angular momentum. The perturbed wave functions are given by

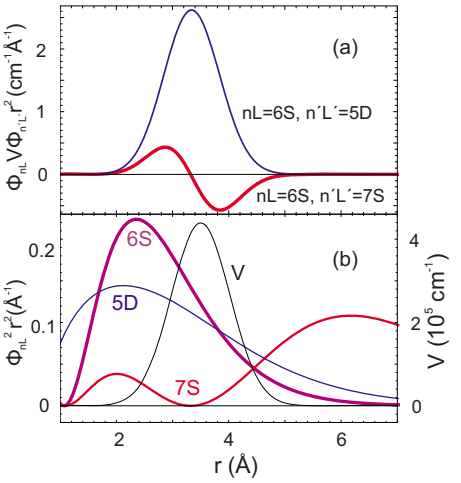

FIG. 5. (Color online) (a) The r dependence of the integrand of Eq. (6), $r^2 \Phi_{6S} V \Phi_{nL}$ for $nL=5D$ (curve 1) and $nL=7S$ (curve 2). (b) Calculated radial probability densities $|\Phi_{nL}|^2(r) r^2$ of $6S$, $5D$, and $7S$ states of Cs [16] and the pseudopotential $V(r)$ [17]. The nucleus of the Cs atom is located at $r=0$, and the He atom is placed at $r=3.5$ Å.

$$|\widetilde{6P_{1/2}}, \pm 1/2\rangle = a(R)|6P, 0, \pm 1/2\rangle + b(R)|6P, \pm 1, \mp 1/2\rangle, \tag{5}$$

where the mixing coefficients $a(R)$ and $b(R)$, with $|a(R)|^2 + |b(R)|^2 = 1$, depend on the radius R of the He ring and where the angular momentum projections M_L, M_S, and M_J are defined with respect to the ring's symmetry axis. In the equilibrium configuration of the exciplex, the ring of He atoms has a radius R of 3.5 Å and the mixing coefficients are found to be $a(R)=0.998$ and $b(R)=-0.069$, respectively. The Cs atom is thus in an almost pure dumbbell-shaped $|6P, M_L=0, M_S\rangle$ state.

In the Franck-Condon approximation the (fluorescing) electronic transition to the $6S_{1/2}$ ground state occurs with the He atoms at fixed positions around the Cs atom. The interaction of the spherically symmetric $6S_{1/2}$ ground state of Cs with the N He atoms located at 3.5 Å is strongly repulsive and is the main reason for the large redshift of the exciplex's transition frequency compared to the corresponding transition in the free atom. The $\widetilde{6S}$ state is strongly perturbed, and its representation requires a larger basis set. For $N=6(7)$ the selection rules imposed by the symmetry of the Hamiltonian imply $\Delta M_L = 0, \pm 6(7), \Delta M_S = 0$, and $\Delta L = 0, \pm 2, \pm 4, \ldots$. We assume that the lowest excited states $5D$ and $7S$ give the dominant contribution to the $\widetilde{6S}$ state, the mixing with P states being forbidden by the selection rules, while the states with $L \geqslant 4$ can be neglected. The relative importance of the contributions from the $7S$ and $5D$ states can be estimated from the following consideration. The interaction is dominated by the Pauli repulsion between the valence electron of the Cs atom and the closed electronic shells of the He atoms. It is modeled by a pseudopotential $V(r)$, as discussed in [17,18]. In Fig. 5(b) we plot the radial probability densities $r^2|\Phi_{nL}(r)|^2$ of the electronic wave functions of the $6S$, $5D$, and $7S$ states calculated in [16] together with the pseudopo-

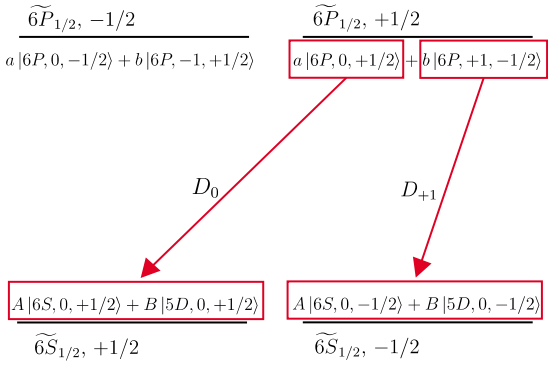

FIG. 6. (Color online) Perturbed states of the Cs atom in the exciplex and electric dipole transitions between the *L*-*S* decoupled components.

tential $V(r)$ from [17]. The nucleus of the Cs atom is located at $r=0$, and the He atom is placed at $r=3.5$ Å. The pseudopotential is nonzero in the volume occupied by the He ring. The wave functions of the states $6S$ and $5D$ have a large overlap in this region, whereas the $7S$ state has a radial node very close to the position of the He ring, so that the matrix element

$$\langle 6S, M_L=0, M_S|V|7S, M_L'=0, M_S\rangle \propto \int \Phi_{6S}(r)V(r)\Phi_{7S}(r)r^2dr \tag{6}$$

practically vanishes as shown in Fig. 5(a). We therefore consider only the admixture of the $5D$ state to $6S$ and represent the $\widetilde{6S}$ state as

$$|\widetilde{6S}_{1/2},\pm 1/2\rangle = A(R)|6S,0,\pm 1/2\rangle + B(R)|5D,0,\pm 1/2\rangle, \tag{7}$$

with $|A(R)|^2+|B(R)|^2=1$.

The states $|\widetilde{6P}_{1/2},\pm 1/2\rangle$ and $|\widetilde{6S}_{1/2},\pm 1/2\rangle$ are both doubly degenerate (Fig. 6), and the selection rule for electric-dipole transitions requires $\Delta M_S=0$. In order to evaluate the lifetime of the perturbed $\widetilde{6P}$ state we have to consider the (polarization-dependent) decays of the states $|\widetilde{6P}_{1/2},\pm 1/2\rangle$ with matrix elements $D_q=\langle \widetilde{6S}_{1/2},\pm 1/2-q|d_q|\widetilde{6P}_{1/2},\pm 1/2\rangle$ of the electric-dipole operator components d_q, where $q=\Delta M_J=0,\pm 1$. Because of symmetry, it is sufficient to consider only the state $|\widetilde{6P}_{1/2},+1/2\rangle$ which has two decay branches with matrix elements

$$\begin{aligned} D_0 &\equiv \langle \widetilde{6S}_{1/2},+1/2|d_0|\widetilde{6P}_{1/2},+1/2\rangle \\ &= a(R)A(R)\langle 6S,0,+1/2|d_0|6P,0,+1/2\rangle \\ &\quad + a(R)B(R)\langle 5D,0,+1/2|d_0|6P,0,+1/2\rangle \\ &= -a(R)A(R)\sqrt{\frac{1}{3}}\langle 6S\|d\|6P\rangle + a(R)B(R)\sqrt{\frac{2}{15}}\langle 5D\|d\|6P\rangle \end{aligned} \tag{8}$$

and

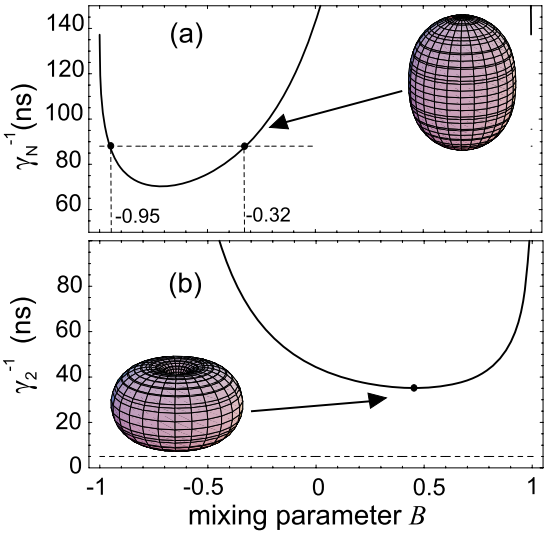

FIG. 7. (Color online) Calculated radiative lifetime of Cs*He$_{N=6,7}$ (a) and Cs*He$_{N=2}$ (b) exciplexes as functions of the $6S$-$5D$ mixing parameter B. Horizontal dashed lines mark the values of τ observed in the experiment. The electronic density distribution of the perturbed $\widetilde{6S}$ state is shown in the insets for (a) $B=-0.32$ and (b) $B=0.45$.

$$\begin{aligned} D_{+1} &\equiv \langle \widetilde{6S}_{1/2},-1/2|d_{+1}|\widetilde{6P}_{1/2},+1/2\rangle \\ &= b(R)A(R)\langle 6S,0,-1/2|d_{+1}|6P,1,-1/2\rangle \\ &\quad + a(R)B(R)\langle 5D,0,-1/2|d_{+1}|6P,1,-1/2\rangle \\ &= b(R)A(R)\sqrt{\frac{1}{3}}\langle 6S\|d\|6P\rangle + b(R)B(R)\sqrt{\frac{1}{30}}\langle 5D\|d\|6P\rangle. \end{aligned} \tag{9}$$

The lifetime time of the $\widetilde{6P}$ state is then given by

$$\frac{1}{\tau(\widetilde{6P}_{1/2},\pm 1/2)} = \frac{1}{3\pi\epsilon_0\hbar c^3}(|D_0|^2+|D_{+1}|^2)\int f(\omega)\omega^3 d\omega, \tag{10}$$

where $f(\omega)$ is the molecular Franck-Condon density and where we assumed that the matrix elements D_q do not vary significantly over the broad exciplex emission spectrum. The expression $f(\omega)\omega^3$ is inferred from the observed spectral line shape $I(\omega)$ shown in Fig. 1 according to

$$f(\omega)\omega^3 = \frac{I(\omega)}{\int \frac{I(\omega)}{\omega^3}d\omega}. \tag{11}$$

Numerical values of the reduced matrix elements for a Cs atom embedded in solid helium are taken from [16] to be $\langle 6P\|d\|6S\rangle=-5.40a_0e$ and $\langle 6P\|d\|5D\rangle=-8.73a_0e$. The radiative lifetime of the Cs*He$_{N=6,7}$ exciplex calculated according to (8)–(10) is plotted in Fig. 7(a) as a function of the mixing coefficient B. For $B=0$ the lifetime is 143 ns. This value is 4 times larger than the free atomic lifetime, due to the ω^3 factor in (10). The observed lifetime is significantly smaller and

corresponds to $B=-0.32$. The second solution ($B=-0.95$), compatible with the experimental result, corresponds to an almost pure $5D$ state in the place of the $6S$ state. In this case the perturbation expansion (7) cannot be applied. The electronic density distribution of the $\widetilde{6S}$ state $|\Psi(r,\theta,\phi)|^2$ can be calculated from

$$\Psi(r,\theta,\phi) = A\Phi_{6S}(r)Y_0^{(0)}(\theta,\phi) + B\Phi_{5D}(r)Y_0^{(2)}(\theta,\phi). \tag{12}$$

We use the radial wave functions and reduced matrix elements of the free Cs atom calculated by the approach described in [18] and discussed in [16]. $|\Psi(r,\theta,\phi)|^2$ corresponding to $B=-0.32$ is shown as an inset in Fig. 7(a). One sees how the spherically symmetric wave function of the unperturbed $6S$ state is squeezed by the ring of n He atoms in the equatorial plane to the shape of an ellipsoid.

2. *Lifetime of the* Cs*He$_{N=2}$ *exciplex*

The Cs($P_{3/2}$)He$_{N=2}$ exciplex contains a Cs atom in one of the degenerate $|6P, M_L=\pm 1, M_S=\pm\frac{1}{2}\rangle$ states which are not mixed with another $|6P, M_L, M_S\rangle$ state. The perturbation Hamiltonian has a $D_{\infty h}$ symmetry and can be represented as

$$V_{\text{Cs-He}} = \sum_{k=0}^{\infty} W_{k,0}Y_0^{(k)}. \tag{13}$$

Using only terms up to $k=2$ the perturbed ground state $\widetilde{6S}$ is described by expression (7) with corresponding A and B. The transition dipole matrix element can be evaluated similarly than for Cs($P_{3/2}$)He$_{N=6,7}$, and the corresponding lifetime is plotted in Fig. 7(b) as a function of the mixing coefficient B. For $B=0$, the factor $\int f(\omega)\omega^3 d\omega$ alone yields a lifetime of 45 ns. The theoretical result of Fig. 7(b) shows that $6S$-$5D$ mixing may reduce this lifetime to a minimal value of 36 ns (at $B=0.45$). The inset in Fig. 7(b) shows the electronic density distribution corresponding to $B=0.45$, where two He atoms located on the symmetry axis, below and above the Cs atom, compress its wave function along the axis. The shortest value of the lifetime is still much larger than the experimental value of $\lesssim$5 ns. We therefore have to conclude that the triatomic exciplex Cs($P_{3/2}$)He$_{N=2}$ is quenched by an additional radiationless process, most likely by its transformation into a larger exciplex with more He atoms.

B. Radiationless processes

The energy structure of the atomic and exciplex states populated by laser excitation at the atomic $6S_{1/2}\rightarrow 6P_{3/2}$ transition is shown schematically in Fig. 8. As discussed earlier [11], the atomic $6P_{3/2}$ state, populated by resonant laser excitation, is completely quenched and does not emit fluorescence. Exciplex formation and fine structure relaxation populating the $6P_{1/2}$ state are responsible for this fluorescence quenching. The decay time of the $6P_{1/2}$ state measured in the present experiment coincides (within experimental errors) with the lifetime measured by Hofer *et al.* [15], when the $6P_{1/2}$ state is directly excited by the laser. This observation shows that the Cs*He$_{N=2}$ exciplex is formed directly

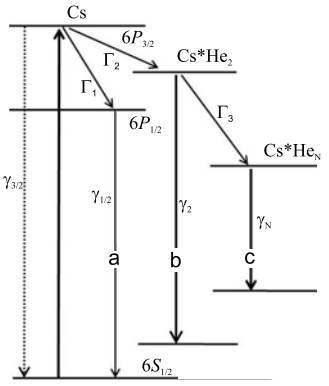

FIG. 8. Level structure of the states involved in the formation and deexcitation of atomic and exciplex states following atomic excitation on the D_2 transition. γ_k denote radiative decay rates, and Γ_k denote radiationless deexcitation rates. The symbols a, b, and c refer to the emission bands of Fig. 1.

from the $6P_{3/2}$ state and that the $6P_{1/2}$ state is not a precursor of the exciplex formation, as shown in Fig. 8.

The ratio of the (spectrally) integrated intensities of the atomic fluorescence, I_{atom}, and of both exciplexes, I_{excip}, gives the relative probabilities of the two channels Γ_1/Γ_2. From Fig. 1 we estimate Γ_1/Γ_2 to be on the order of $\simeq 10^{-2}$. The decay rates Γ_1 and Γ_2 are much larger than the radiative decay rate ($\gamma_{3/2}$) of the $6P_{3/2}$ state, which should be comparable to the radiative rate ($\gamma_{1/2}$) of the $6P_{1/2}$ state. Exciplex formation rates in the range of 100 ps were reported [6,9] for Na, K, and Rb on He nanodroplets, excited at the corresponding atomic D_2 transitions. We therefore expect subnanosecond rise times of the atomic and exciplex fluorescence pulses, which cannot be resolved with the relatively long excitation laser pulse in the present experiment.

The model presented in Sec. III A predicts a lower limit $\gamma_2^{-1} \geqslant 36$ ns for the *radiative* lifetime of Cs*He$_{N=2}$. From the measured fluorescence pulse shape (Fig. 3) we conclude that the experimental decay time is much shorter than that calculated lower limit. It is thus reasonable to assume that the Cs*He$_{N=2}$ exciplex is quenched by a *radiationless* transformation into the larger Cs*He$_{N=6,7}$ complex through the attachment of additional He atoms. The rate of that process is denoted by Γ_3 in Fig. 8. We can estimate the rate of formation of Cs*He$_{N=6,7}$ as follows. Assuming that Cs*He$_{N=6,7}$ cannot be formed from the $6P_{3/2}$ state directly, but only via the intermediate Cs*He$_{N=2}$ complex, one can estimate the ratio of the two relaxation rates of Cs*He$_{N=2}$ from the relative intensities of the (total) fluorescence emitted by the two exciplexes:

$$\frac{\Gamma_3}{\gamma_2} = \frac{I_{N=6,7}}{I_{N=2}} \simeq 4.5. \tag{14}$$

Using Eq. (14) and the calculated minimum value for the radiative lifetime of Cs*He$_{N=2}$ one obtains a lower limit for the rate of the Cs*He$_{N=6,7}$ exciplex formation, $\Gamma_3 \leqslant 1.3 \times 10^9$ s^{-1}. On the other hand, one can estimate Γ_3 from the measured total decay time of the Cs*He$_{N=2}$ fluorescence,

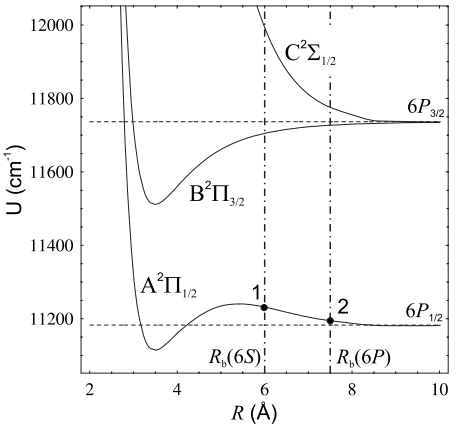

FIG. 9. Potential energy diagram of the linear Cs*He$_2$ exciplex. Each of the two helium atoms is separated from the Cs atom by the distance R. Vertical dash-dotted lines show the radii of the atomic bubbles formed by the $6S_{1/2}$ and $6P_{1/2}$ states of Cs atom in solid He.

$$\tau(\mathrm{Cs^*He}_{N=2}) = \frac{1}{\gamma_2 + \Gamma_3} \leqslant 5 \text{ ns}, \qquad (15)$$

which yields $\Gamma_3 \geqslant 1.7 \times 10^9$ s^{-1}. The small discrepancy between the two values is acceptable considering the approximations involved in the determination of γ_2: the excited $6P$ state is treated as unperturbed, the expression for the perturbed ground $6S$ state includes only two contributions from the unperturbed $6S$ and $5D$ states, and the dependence of the transition dipole matrix element on the Cs-He separation (He-ring radius) is assumed to be weak, so that the factor $(D_0^2 + D_{-1}^2)$ can be taken out of the integrand in Eq. (8). The fact that the two estimates of Γ_3 yield comparable bounds leads us to conclude that the formation rate Γ_3 is in the range of $(1-2) \times 10^9$ s^{-1}; i.e., the exciplex formation time is in the range of 0.5–1 ns.

C. Dynamics after D_1 excitation

After excitation at the atomic D_1 transition, the Cs*He$_{N=2}$ exciplex is formed in the $A\,^2\Pi_{1/2}$ state, correlating to the $6P_{1/2}$ atomic asymptote. The corresponding potential curve from [11] is shown in Fig. 9. In order to form the quasibound complex, He atoms have to tunnel under the potential barrier at R=5.5 Å. Because of this barrier, exciplex formation is strongly suppressed and the excited Cs atoms decay preferentially by fluorescence emission at the atomic D_1 transition with a lifetime $\tau(6P_{1/2})$=29 ns [15]. On the other hand, it is known [18,19] that the excitation of a Cs atom in liquid or solid He is followed by a very fast (picosecond time scale) rearrangement of He atoms around it. The ground-state Cs atom resides in a spherical cavity (atomic bubble) with a radius $R_b(6S)$=6.0 Å. After the excitation, the bubble expands up to $R_b(6P)$=7.5 Å to accommodate the more extended $6P_{1/2}$ state wave function and the fluorescence is emitted from this larger bubble [20]. The question therefore arises as to whether the exciplex formation occurs in the large bubble or during the bubble expansion.

In Fig. 9 one sees that in the initial bubble configuration the He atoms on the bubble interface are located much closer to the top of the potential barrier (point 1 in Fig. 9) than in the expanded bubble (point 2 in Fig. 9). The probability of a tunneling transition and thus of exciplex formation is therefore significant only during the first instants (ps or less) after the excitation. It quickly decreases as the bubble expands towards the equilibrium radius $R_b(6P)$ and can thus no longer affect the lifetime of the $6P_{1/2}$ state in the expanded bubble. The present experimental results are compatible with this scenario. The observed fluorescence of the Cs($6P_{1/2}$)He$_{N=2}$ exciplex vanishes immediately after the laser pulse, much faster than the decay time of the atomic $6P_{1/2}$ state. This supports the assumption that the branching to the exciplex occurs only in the very beginning of the relaxation process and that the probability of the tunneling transition in the large bubble is negligible.

IV. SUMMARY

We have presented time-resolved studies of the different decay channels of laser-excited Cs($6P_{1/2,3/2}$) atoms in a solid He matrix. We have presented evidence that the linear Cs*He$_{N=2}$ exciplex is a transient product in the formation of a terminal ring-shaped Cs*He$_{N=6,7}$ exciplex. We have also measured the radiative decay time of Cs*He$_{N=6,7}$, which is approximately 3 times longer than that of the corresponding excited state of the Cs atom. This effect is mainly due to the large redshift of the exciplex emission wavelength with respect to the atomic fluorescence. However, the analysis of the lifetime also reveals a significant effect of the Cs-He interaction on the transition dipole matrix element which is larger than in the free Cs atom. We describe this enhancement in terms of a He-induced mixing of S and D states.

ACKNOWLEDGMENT

This work was supported by Grant No. 200021-111941 of the Swiss National Foundation.

[1] K. Enomoto, K. Hirano, M. Kumakura, Y. Takahashi, and T. Yabuzaki, Phys. Rev. A **66**, 042505 (2002).
[2] K. Hirano, K. Enomoto, M. Kumakura, Y. Takahashi, and T. Yabuzaki, Phys. Rev. A **68**, 012722 (2003).
[3] K. Enomoto, K. Hirano, M. Kumakura, Y. Takahashi, and T. Yabuzaki, Phys. Rev. A **69**, 012501 (2004).
[4] J. Reho, C. Callegari, J. Higgins, W. E. Ernst, K. K. Lehmann, and G. Scoles, Faraday Discuss. **108**, 161 (1997).
[5] J. Reho, J. Higgins, C. Callegari, K. K. Lehmann, and G. Scoles, J. Chem. Phys. **113**, 9686 (2000).
[6] J. Reho, J. Higgins, K. K. Lehmann, and G. Scoles, J. Chem. Phys. **113**, 9694 (2000).

[7] F. R. Brühl, R. A. Trasca, and W. E. Ernst, J. Chem. Phys. **115**, 10220 (2001).
[8] C. P. Schulz, P. Claas, and F. Stienkemeier, Phys. Rev. Lett. **87**, 153401 (2001).
[9] G. Droppelmann, O. Bünermann, C. P. Schulz, and F. Stienkemeier, Phys. Rev. Lett. **93**, 023402 (2004).
[10] D. Nettels, A. Hofer, P. Moroshkin, R. Müller-Siebert, S. Ulzega, and A. Weis, Phys. Rev. Lett. **94**, 063001 (2005).
[11] P. Moroshkin, A. Hofer, D. Nettels, S. Ulzega, and A. Weis, J. Chem. Phys. **124**, 024511 (2006).
[12] A. Hofer, P. Moroshkin, D. Nettles, S. Ulzega, and A. Weis, Phys. Rev. A **74**, 032509 (2006).
[13] M. Arndt, R. Dziewior, S. Kanorsky, A. Weis, and T. Hänsch, Z. Phys. B: Condens. Matter **98**, 377 (1995).
[14] P. Moroshkin, A. Hofer, S. Ulzega, and A. Weis, Fiz. Nizk. Temp. **32**, 1297 (2006) [J. Low Temp. Phys. **32**, 981 (2006)].
[15] A. Hofer, P. Moroshkin, S. Ulzega, and A. Weis, Eur. Phys. J. D **46**, 9 (2008).
[16] A. Hofer, P. Moroshkin, S. Ulzega, and A. Weis, Phys. Rev. A **77**, 012502 (2008).
[17] J. Pascale, Phys. Rev. A **28**, 632 (1983).
[18] A. Hofer, P. Moroshkin, S. Ulzega, D. Nettels, R. Müller-Siebert, and A. Weis, Phys. Rev. A **76**, 022502 (2007).
[19] T. Kinoshita, K. Fukuda, Y. Takahashi, and T. Yabuzaki, Phys. Rev. A **52**, 2707 (1995).
[20] Note that the equilibrium radii given here were calculated on the basis of the pseudopotential approach discussed in [16]. The values reported here are more reliable than our previously published values [11] obtained from a pair potential approach.